Supplemental Information

A Model sensitivity

We showed in the main text how altering the parameters of the individual-based model (IBM) can switch the model output between three different qualitative states: the infection dies out, all non-carrier leafhoppers die out, or populations of carrier and non-carrier leafhoppers are maintained simultaneously. Here we first demonstrate that changing virulence or transmission has no impact on the qualitative characteristics of the ordinary

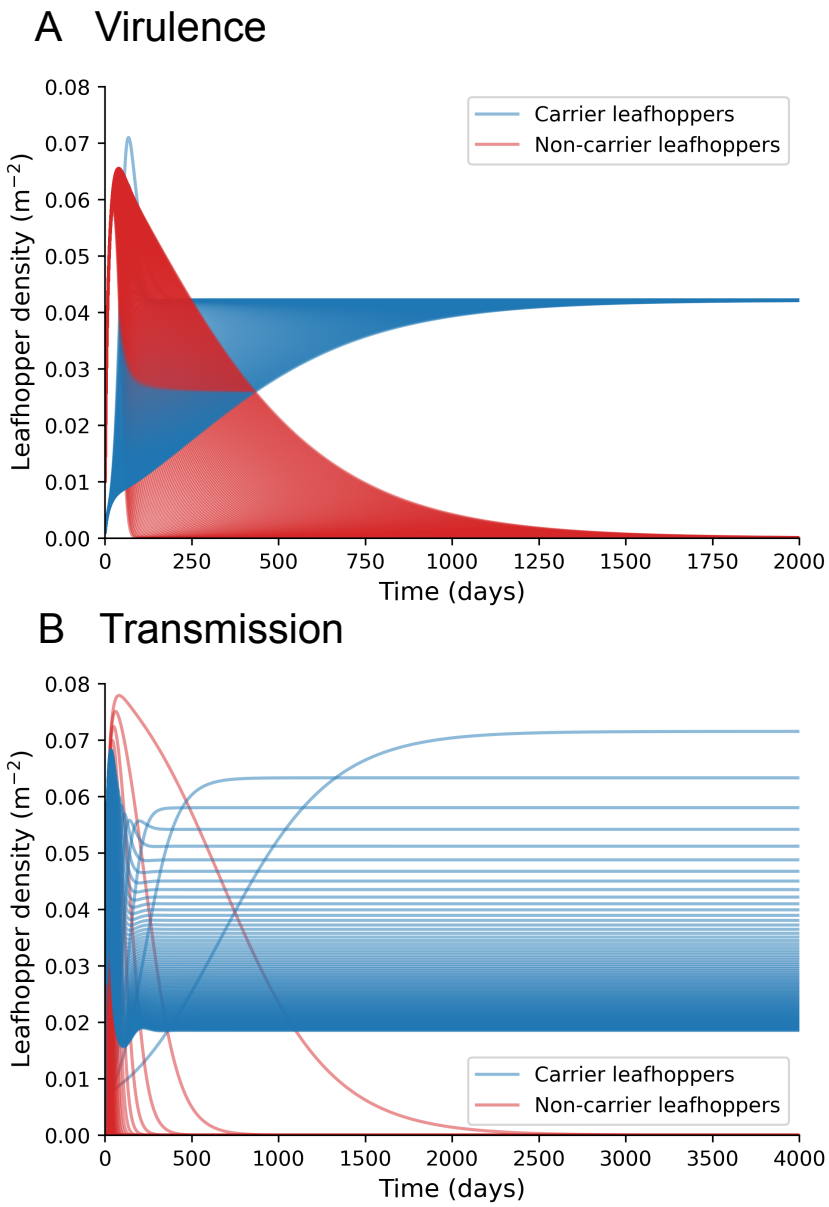

Figure S1. Robustness of ODE model. The defining characteristic of the ODE model predictions, namely that all non-carrier leafhoppers die out, is not affected by changes to (A) virulence or (B) transmission. The range of numerical values spanned for the three parameters were between 0.01 and 1, in increments of 0.01 (with units d^{-1} and $\mathrm{m}^2\,\mathrm{d}^{-1}$, respectively); virulence m_H was varied independently, while transmissions β_H and β_L were varied conjointly.

differential equation (ODE) model output. Figure S1A shows that varying virulence (m_H) between 0.01 and 1 d^{-1} (in increments of 0.01) has no impact on the model behaviour. Over relatively long timescales, the predicted carrier leafhopper density reaches the same steady state value. Figure S1B shows that varying transmission (β_H, β_L) results in the same qualitative output, namely that non-carrier leafhopper populations systematically die out, even though the steady state predictions for the carrier leafhopper population do depend on the specific choice of β_H and β_L (both parameters were varied conjointly between 0.01 and 1 $m^2\,d^{-1}$ in increments of 0.01).

B Comparing the ODE and IBM implementations

B.1 A fair comparison: why we need one, and how we did it

The central hypothesis of this study is based on the assumption that accurately representing the dynamics of a vector-spread pathogen outbreak requires a model that can explicitly handle space. Furthermore, the impact of space can be investigated, both quantitatively and qualitatively, by comparing models that are identical in all ways bar their treatment of space. We selected a population-based model, formulated as a set of coupled ordinary differential equations (ODEs), to compare with an equivalent individual-based model (IBM) that represents individual leafhoppers as particles, moving across a landscape of grid cells containing a density of plant hosts. This comparison, however, is only informative about the contribution of space if we can guarantee that all other differences between the models have been appropriately dealt with, such that the models behave similarly at the well-mixed (reshuffled) limit. This requires careful calibration, given that ODE models and IBMs are very different model formalisms. IBMs include stochasticity, discrete populations of individuals, and often a discretisation of space, while ODEs are deterministic, well-mixed and capturing continuous variables. Moreover, the dynamics of IBMs are event-based, while those of ODEs are time-based. In order to have a fair comparison between the IBM and the ODE model, it is therefore important to have an implementation of the stochastic processes that gives rise to matching deterministic dynamics under certain limiting conditions. Moreover, it is critical to look at the discretisation of variables and space within the IBM, which can introduce artefacts as well. Besides, the spatial coupling, through both the density-dependent mortality and leafhopper movement, can introduce additional mismatches, even within the reshuffled setting. We therefore designed a series of simulations to detect other possible sources of disparity between the IBM and the ODE model and to then use these insights to fine-tune the IBM model parameterisation as to guarantee a close match at the well-mixed (reshuffled) limit.

B.2 Discretisation of variables and space

The first possible source of mismatch that we tackle is the field size. Large fields contain in total high numbers of leafhoppers, resulting in a law of large numbers driving the impact of stochasticity to become negligible. In contrast, small simulated field sizes can impact model results due to a same leafhopper density now corresponding to a much smaller total number of leafhoppers, giving rise to large stochastic fluctuations. In order to explore this effect, we simulated a field consisting of only a single grid cell. This unique grid cell was then varied in size (with the total field size thus varying accordingly), in order to determine the minimal field size at which a good agreement between the IBM and ODE

model can be established. Note that by using a single grid cell the simulation effectively becomes 'well-mixed', given that within the IBM the effect of leafhoppers on plant hosts and vice-versa are both evaluated at the level of the grid cell.

Figure S2 shows the evolution of carrier leafhopper density over time for different grid cell sizes (and thus field sizes). Convergence between the IBM and ODE model can be observed for field sizes larger than 256 m×256 m. For intermediate field sizes (of 64 m×64 m to 128 m×128 m), strong fluctuations in the leafhopper density can be observed, due to the stochastic nature of the simulations combined with low leafhopper numbers, with those fluctuations increasing for decreasing field sizes. Nevertheless, for those sizes the equilibrium dynamics remain preserved, with fluctuations consistently around the ODE prediction. Their initial transient behaviours, however, can present deviations from the ODE model. In contrast, at field sizes smaller than 32 m×32 m the carrier leafhopper populations collapse, due to an even further increased impact of stochasticity combined with the existence of an absorbing boundary (because once all infection and/or all leafhoppers are lost, they can not reappear). The good agreement with the ODE model at large field sizes confirms that the IBM is capturing well and in a comparative manner the basic interactions of the system as described in the ODE. These results also highlight the impact of stochasticity within the IBM formalism at medium and small field sizes due to low leafhopper numbers, even within this specific context in

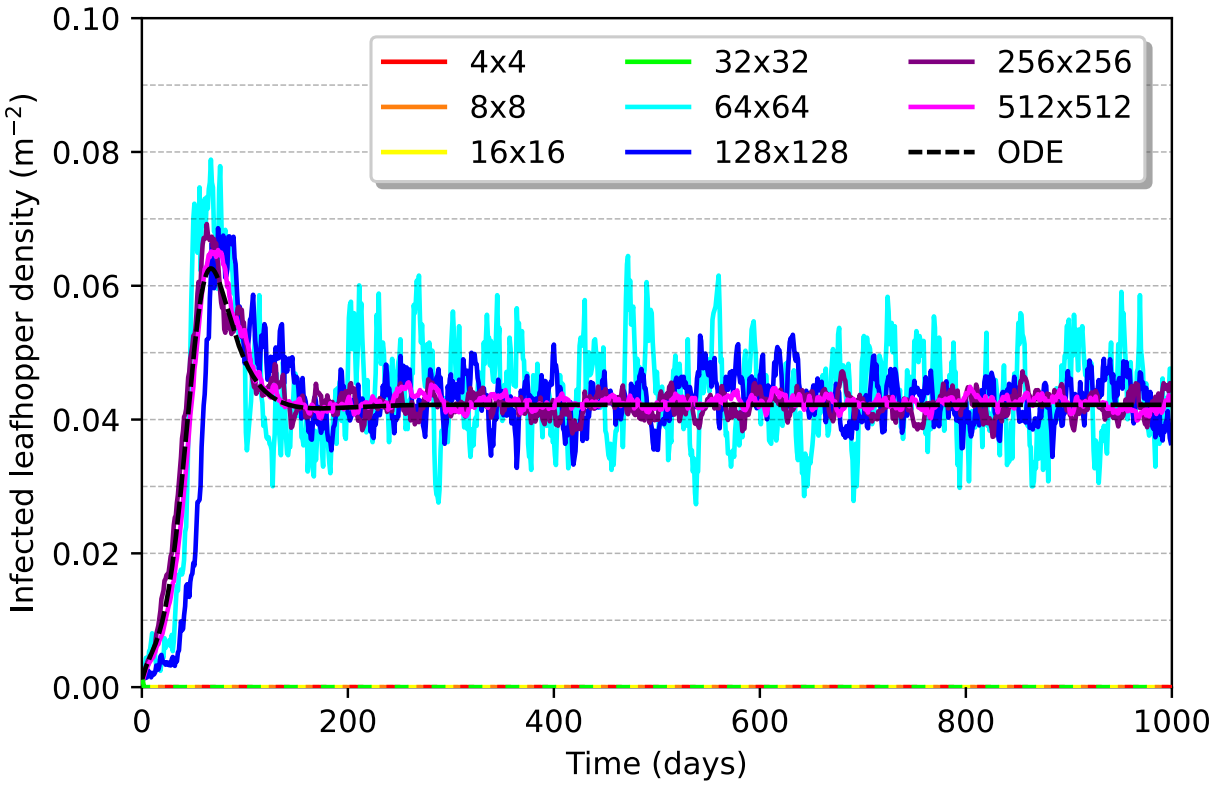

Figure S2. The impact of stochasticity at small field sizes. When the simulated field size is reduced, an increasing IBM sensitivity to noise can be observed, due to decreasing overall leafhopper numbers. All fields are comprised of a single grid cell, which is reduced in size from 512 m×512 m to 4 m×4 m, as indicated. ODE dynamics are shown by the black dashed line. For field sizes smaller than 32 m×32 m, the infection rapidly dies out, due to the high levels of stochasticity causing the dynamics to hit the absorbing boundary.

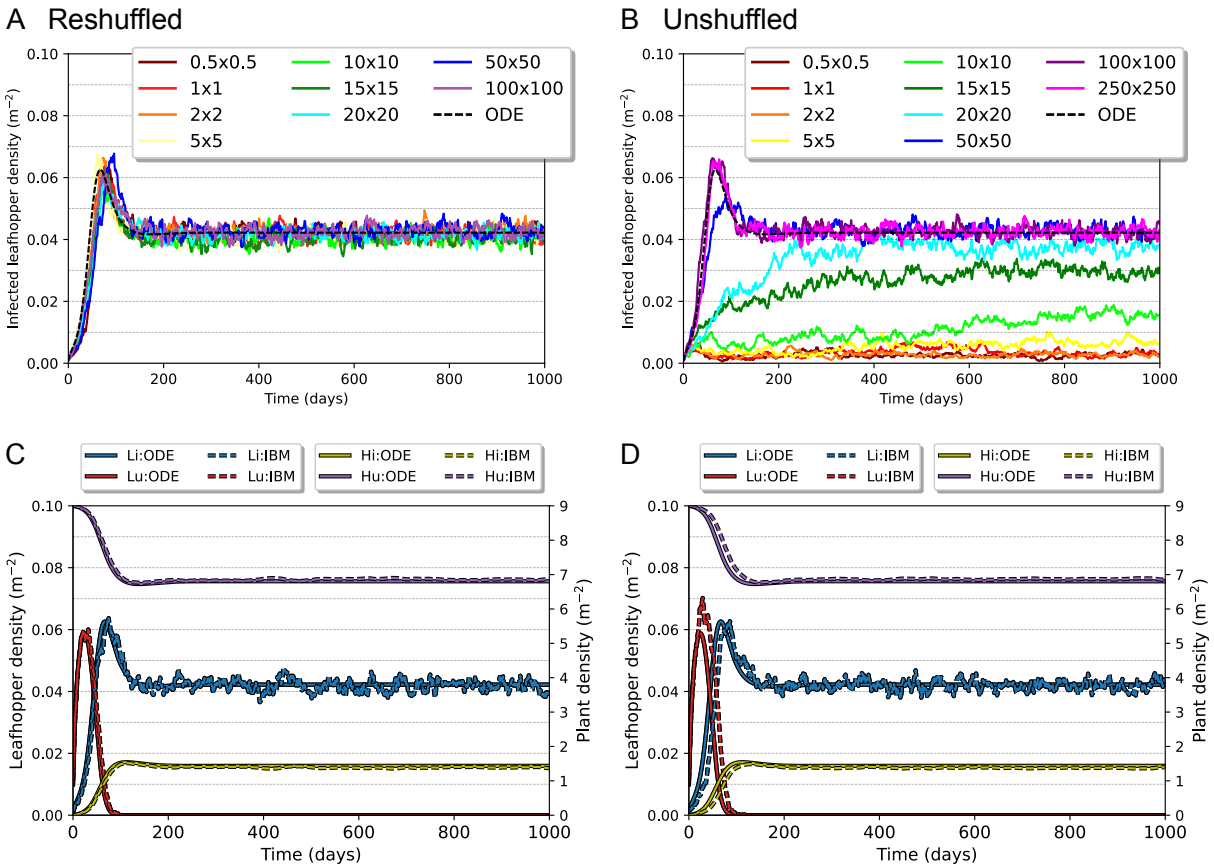

Figure S3. Impact of grid cell size on reshuffled and unshuffled IBM simulations. Carrier leafhopper time dynamics for different plant host grid cell sizes in either reshuffled (A) or unshuffled (B) IBM simulations. Depicted are the average carrier leafhopper density over the whole field for simulations with varying grid cell size, as indicated. (C, D) Comparison between reshuffled IBM and ODE model for plant host grid cell size of 1 m×1 m (C) and 0.5 m×0.5 m (D).

which spatial patterns are excluded by simulating a single grid cell only. Based upon these results, a default field size of 400 m×300 m was chosen.

The standard IBM implementation however does not use a single grid cell, but instead discretises space (the field) into a large number of plant host grid cells ('grid cells'), and so the next step was to determine the impact of this discretisation. Figure S3 shows the carrier leafhopper dynamics when the field is represented by a collection of grid cells of varying size. Figure S3A shows the impact of grid cell resolution while excluding spatial patterning by means of reshuffling the grid cells and leafhoppers after each simulation time step, while Figure S3B shows the same simulations whilst allowing for spatial patterning to emerge by turning off the reshuffling.

When the grid cells are being reshuffled, our expectation is be that the IBM would behave alike the ODE model. This is indeed the case of a wide range of grid cell sizes. Indeed, at large grid cell sizes (100 m×100 m) the ODE limit is achieved by the IBM due to the large numbers of particles contained in each of the few and large grid cells (Figure S3A, purple line). This way of matching the ODE dynamics is similar to what was observed in the simulations presented in Figure S2 for large grid sizes, and is therefore biologically less relevant, as it precludes any spatial patterning. At intermediate grid cell sizes (5 m×5 m to 50 m×50 m) slightly larger fluctuations ensue, due to the combined effect

of the stochasticity within each grid cell and the coarseness of the field resolution (not too many grid cells per field). However, at small grid cell sizes (1 m×1 m to 2 m×2 m), the IBM dynamics again very closely approach the ODE model (Figure S3C and Figure 2C). Despite the grid cells being small and individually harbouring larger fluctuations then the intermediate grid cells, this source of stochasticity is overshadowed by the far larger total number of grid cells, with the average behaviour of the grid ensemble bringing the IBM back again to the ODE limit. Finally, at tiny grid cell sizes (of less than 0.5 m×0.5 m), there is a lower limit at which the large density variations within each grid cell (with even the entering or leaving of a single leafhopper into a grid cell already causing huge changes in the local leafhopper density, strongly impacting the grid cell dynamics) cause the absorbing boundary to be hit more often, resulting in yet again increasing fluctuations (Figure S3D). Nevertheless, within the reshuffled setting a consistent good correspondence between IBM and ODE model can be observed. Repeating these simulations within the unshuffled setting, we observe different behaviour, which we can contribute to the spatial patterning (Figure S3B). Similarly as in Figure S3A, at large grid cell sizes (larger than 100 m×100 m) the ODE dynamics are matched, due to the fact that at this limit each individual grid cell is again within the well-mixed domain. At intermediate grid cell sizes (of 15 m×15 m to 20 m×20 m) we observe increased fluctuations in the carrier leafhopper density. In contrast to the reshuffled setting, this is however combined with clearly reduced levels of carrier leafhoppers as well as increased transient time-scales of non-carrier leafhopper survival. At small grid sizes (of 0.5 m×0.5 m to 5 m×5 m), the spatial patterning allows for the structural co-existence of carrier and non-carrier leafhoppers as well as a the fraction of carrier leafhoppers dropping to low levels (which is the behaviour that we extensively discuss in this paper). It is within these settings that the spatial patterning is allowed to manifest itself and impact the dynamics in a biologically meaningful manner.

B.3 Spatial coupling

The spatial coupling, through both density-dependent mortality of leafhoppers and leafhopper movement, can introduce additional mismatches between the IBM and ODE model, even within the reshuffled setting. The impact of different motility rates will be discussed in detail in section C.3. Here we focus on the density-dependent mortality, which represents leafhopper losses due to predation. This function is non-linear to account for typical search image and prey-switching behaviour (Akre and Johnson, 1979). That is, a large local leafhopper density is more likely to attract predators. It is assumed that such density-dependent mortality acts over a scale that is larger than the individual plant host grid cells, but also not on a global scale, as this process involves locally attracting predators (and/or locally increasing parasite/disease propagation, which is another mechanism causing density-dependent mortality). The area over which this interaction occurs reflects the behaviour of the leafhopper predators. Because those predators are not explicitly modelled, a biologically reasonable shortcut is required. For example, if the density-dependent predation were assumed to be homogenous over the entire field, this would imply that a large density of leafhoppers within a single grid cell could affect predation over the entire 300 m×400 m area, such an assumption would not be biologically reasonable. Another extreme implementation would be a that the density-dependent mortality acts on the scale of the individual grid cell only. This would result in uncorrelated predation pressure for each grid cell, typically assumed to be 2 m×2 m. Given

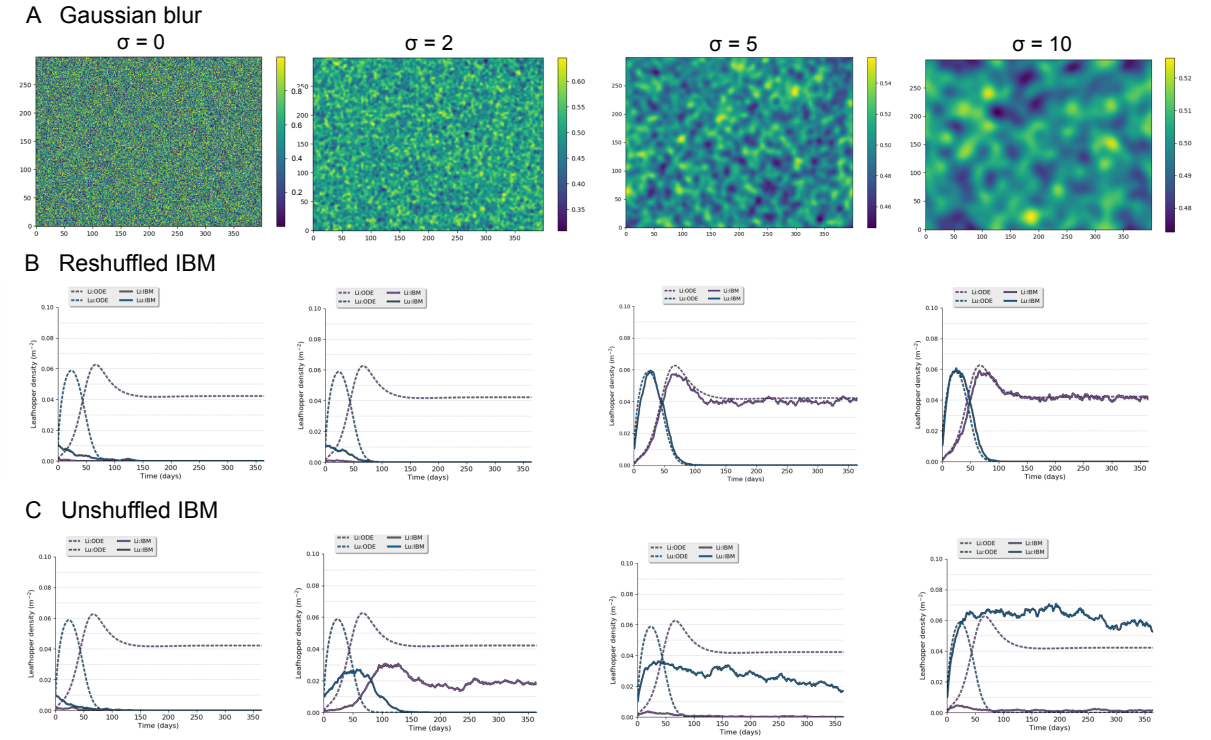

Figure S4. Effect of the breadth of the spatial coupling in the density-dependent mortality. The IBM model predictions are sensitive to the parameterisation of the gaussian blur in the density-dependent mortality function. (A) A field of 300×400 m filled with random values between 0 and 1, with subsequently a gaussian blur applied to the data using σ values of 0, 2, 5, and 10 m, demonstrating how the smoothing is influenced by σ. (B, C) The impact of σ on the model dynamics of the reshuffled (B) and unshuffled (C) IBM.

typical search distances for insect predators such as birds (Bell, 2012), this would again be biologically unreasonable. Thus, the most realistic scenario lies somewhere between those two extremes. We therefore tested how the reach of the spatial coupling in predation could impact the dynamics of the model, using both the reshuffled and the unshuffled, spatially explicit IBM.

A gaussian leafhopper interaction kernel was used to calculate the effective leafhopper density at any local position, to be used then in the density-dependent mortality probability. A range of different sigma values, which define the width of the gaussian kernel, were tested. Figure S4 shows the results for a range of values (σ = 0, 2, 5 and 10 m). These values determine the spread of the effective predation, as depicted in Figure S4A. The corresponding impact on the dynamics of the reshuffled IBM is shown in Figure S4B, and of the unshuffled (spatially explicit) IBM in Figure S4C.

When the IBM is reshuffled, we observe that when spatial coupling is non-existent or very small (σ=0 or 2) all leafhoppers die out (Figure S4B, first two panels). This is because the predation pressure is locally very high whenever there are leafhoppers present. Increasing the spatial spread, to σ=5 or 10 causes the reshuffled IBM behaviour to become more and more similar to the ODE model (Figure S4B, last two panels). At σ=5, the effect of increased local predation pressure can be still be observed, as the leafhopper population still keeps a bit below the ODE level; when the spatial coupling distance is increased to σ=10, we however find the IBM population levels fluctuating right on top of the ODE line.

For the spatially explicitly IBM, σ=0 still results in all leafhoppers dying out (Figure S4C, first panel). At the other extreme, for the larger kernel widths of σ=5 and 10, we now observe the typical mixed population levels that ensue when spatial patterning is allowed to occur (Figure S4C, last two panels). Similarly to the well-mixed scenario, at σ=5 leafhopper populations are lower than at σ=10, due to the increased local predation pressure (Figure S4C, compare third to forth panel). Interestingly, when the predation pressure is locally high due to a too small kernel width of σ=2, it causes a too high disruption to the spatial patterning, given the effective locally increased mortality, thereby giving rise to dynamics that are much closer to the results of the ODE model (in which infection dominates and non-carrier leafhoppers die out).

Taking this all into account, our model uses as the default value $\sigma = 10$. Larger values were considered to be biologically less reasonable, given its mechanistic implications for the predator-prey interactions, but would not quantitatively affect the results.

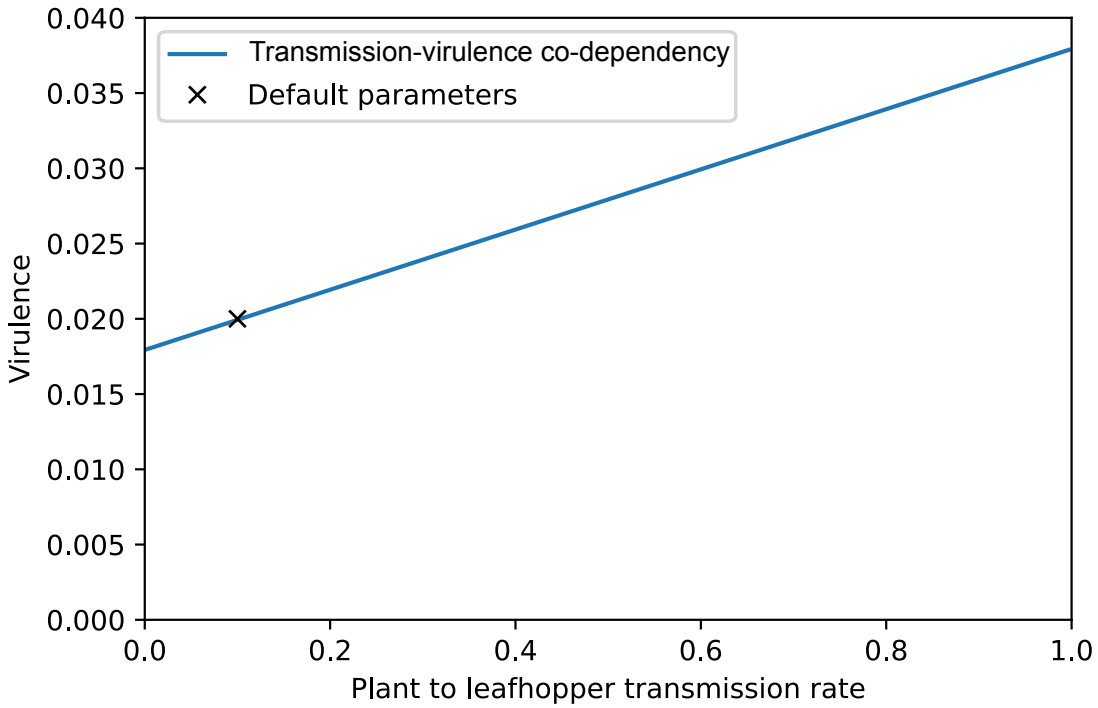

Figure S5. Transmission and virulence co-dependency on severity as used in the competition experiments. The competition experiments in the main text show how pathogens of differing severities, Severity 1 and Severity 2, outcompete each other. Severity, as shown along both the x- and y-axes in Figure 4, ranges from 0 to 10. Depicted is the associated transmission and virulence over that severity interval. The parameters used to translate severity into transmission and virulence are $\beta_{Ls} = 0.1, m_{Ho} = 0.018, m_{Hs} = 0.002$, which translates into transmission values β_L between 0 and 1 $\mathrm{m^2\,Plant^{-1}\,d^{-1}}$and virulence values between 0.018 and 0.038 $\mathrm{d^{-1}}$.

C Competition experiments

C.1 Defining pathogen severity in terms of transmission and virulence

Traditional trade-off hypotheses of pathogen evolution assume that there is a high correlation between transmission and virulence, since factors that increase transmission, such as pathogen load, in general also concurrently increase virulence (Anderson and May, 1982). We introduce pathogen severity as an evolvable trait, which determines both virulence and transmission. Transmission (β_L) and virulence (m_H) increase in a linear fashion with the dimensionless pathogen severity S in the following way: $\beta_L = \beta_{Ls}S$; $m_H = m_{Ho} + m_{Hs}S$, where m_{Ho} and β_{Ls}, m_{Hs} are positive parameters capturing respectively the offset and slopes of these relationships. High severity is thus represented by both high transmission and high virulence. Given that no virulence is observed in the carrier leafhoppers themselves, while the virulence for the plant hosts can be large, we here focus on the joint evolution of plant-to-leafhopper transmission and virulence for the plant hosts in terms of severity, while assuming zero impact on leafhopper survival and their capability to infect plants. We furthermore assume that plant host virulence can never be entirely absent, as this would be inconsistent with AYp being a plant pathogen. Figure S5 depicts this fixed relationship between virulence and transmission as used in the main study. An increase in severity can be viewed as moving from the left to the right along the line shown in the figure.

C.2 Model sensitivity and robustness with respect to the transmission-virulence co-dependency relationship

Figure S6 shows how the results of the competition experiments change when the co-dependency between transmission and virulence is modified from the relationship as was used for Figure 4 (Figure S5, Figure S6A, blue line, y1). When, compared to the default relationship, virulence rises more sharply with increasing transmission (see Figure S6A, green line, y2, with the default parameters still part of the transmission-virulence relationship), infections die out at both lower severity levels, due to lack of transmission, and higher severity levels, due to high virulence destroying the vector's resource (Figure S6B). Only for a small range of intermediate severity levels, mixed populations of carrier and non-carrier can be observed. A too severe impact of the transmission on the virulence level thus renders the pathogen dynamics structurally at the edge of extinction, which seems to be biologically unreasonable. In contrast, when virulence only weakly rises with increasing transmission (see Figure S6A, red line, y3, with the default parameters again still part of the transmission-virulence relationship), then the patterning remains highly comparable with the results as presented in Figure 4B of the main text (Figure S6C). When the rise is more shallow, however, we observe that the selection strength for a specific severity also becomes weaker, causing more prolonged periods of co-existence between different strains. Nevertheless, the qualitative outcomes of evolution towards lower severity, mixed carrier and non-carrier populations and spatio-temporal patterning remains conserved. When the slope in the co-dependency between transmission and virulence is preserved, but the virulence offset is lowered (Figure S6A, purple line, y4), a highly comparable picture arises as presented in Figure 4B (Figure S6D), with however evolutionary dynamics towards even lower severity, as well as stronger selective pressures

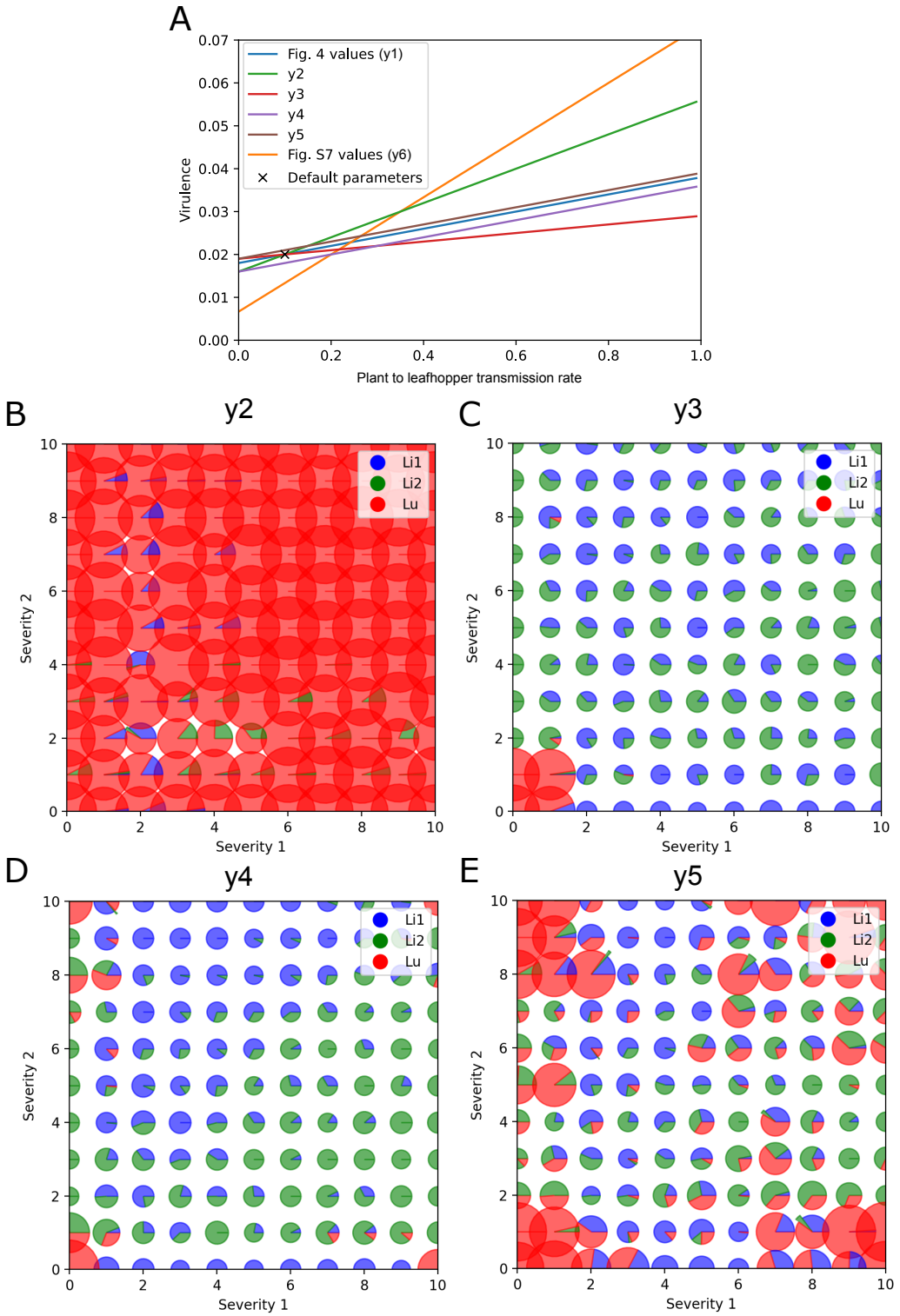

Figure S6. The impact on the evolutionary dynamics of the particular co-dependency relationship between virulence and plant-to-leafhopper transmission. (A) Alternative co-dependencies between transmission and virulence. Relationships between transmission and virulence are labelled y1–y7. Default settings as used in Figure 4 (y1): $\beta_{Ls} = 0.1, m_{Ho} = 0.018, m_{Hs} = 0.002$; y2: $\beta_{Ls} = 0.1, m_{Ho} = 0.016, m_{Hs} = 0.004$; y3: $\beta_{Ls} = 0.1, m_{Ho} = 0.019, m_{Hs} = 0.001$; y4: $\beta_{Ls} = 0.1, m_{Ho} = 0.016, m_{Hs} = 0.002$; y5: $\beta_{Ls} = 0.1, m_{Ho} = 0.019, m_{Hs} = 0.002$. Alternative setting to demonstrate evolutionary robustness, as used in Figure S7 (y6): $\beta_{Ls} = 0.1, m_{Ho} = 0.0067, m_{Hs} = 0.0067$. (B–E) Outcome of competition experiments for severity relationships y2–y5.

between different strains. Conversely, increasing the virulence offset (Figure S6A, brown line, y5) drives the evolutionary dynamics towards slightly higher severity, while high severities now trigger extinction of the pathogen, again due to too high virulence levels, but again not changing the qualitative evolutionary outcome (Figure S6E). Finally, the deviating results in Figure S6B are not due to the steepness in the transmission-virulence co-dependency. To illustrate this, we will show in Figure S7 below the results of the competition experiments when using an even steeper relationship, but now counterbalanced by a lower offset in virulence (Figure S6A, orange line, y6). The same qualitative evolutionary outcomes ensue. Together, these results show that as long as the dynamics do not trigger the complete extinction of the pathogen, the qualitative evolutionary outcomes of severity selection are robust to the specific choice of the transmission-virulence co-dependency. Note, however, that the precise point of the ESS in terms of transmission and virulence can quantitatively shift whilst remaining stable.

C.3 Impact of leafhopper movement on the evolutionary dynamics

Several of the phytoplasma effector proteins are known to affect leafhopper movement. We therefore hypothesised that changes to leafhopper movement might have a pronounced quantitative impact on the parameter setting at which the evolutionarily stable strategy (ESS) would be reached. The reasoning is that such a sensitivity would warrant a high diversity in those effector proteins in between pathogen strains, as to allow for fast adaptation to changing environmental condition, as discussed in the main text. We therefore tested this by running the competition experiments for a range of different movement values (2.9, 3.0, 3.1, 3.2 $\mathrm{m\,d^{-1}}$). Figure S7 indeed shows sensitivity to leafhopper motility, with for higher motility a strong reduction in the severities for which we would expect the pathogen to survive, as well as a weak increase in the severity at the ESS. Nevertheless, the qualitative pattern, stability of the QSS, evolution to co-existence of carrier and non-carrier leafhoppers, and evolution towards spatio-temporal patterning are all preserved. As discussed above, we here used a different transmission-virulence relationship to illustrate the qualitative robustness of the competition dynamics (compare Figure S7B with Figure 4B). Note that the qualitative features of the depicted sensitivity to leafhopper movement is however independent of the specific transmission-virulence co-dependency.

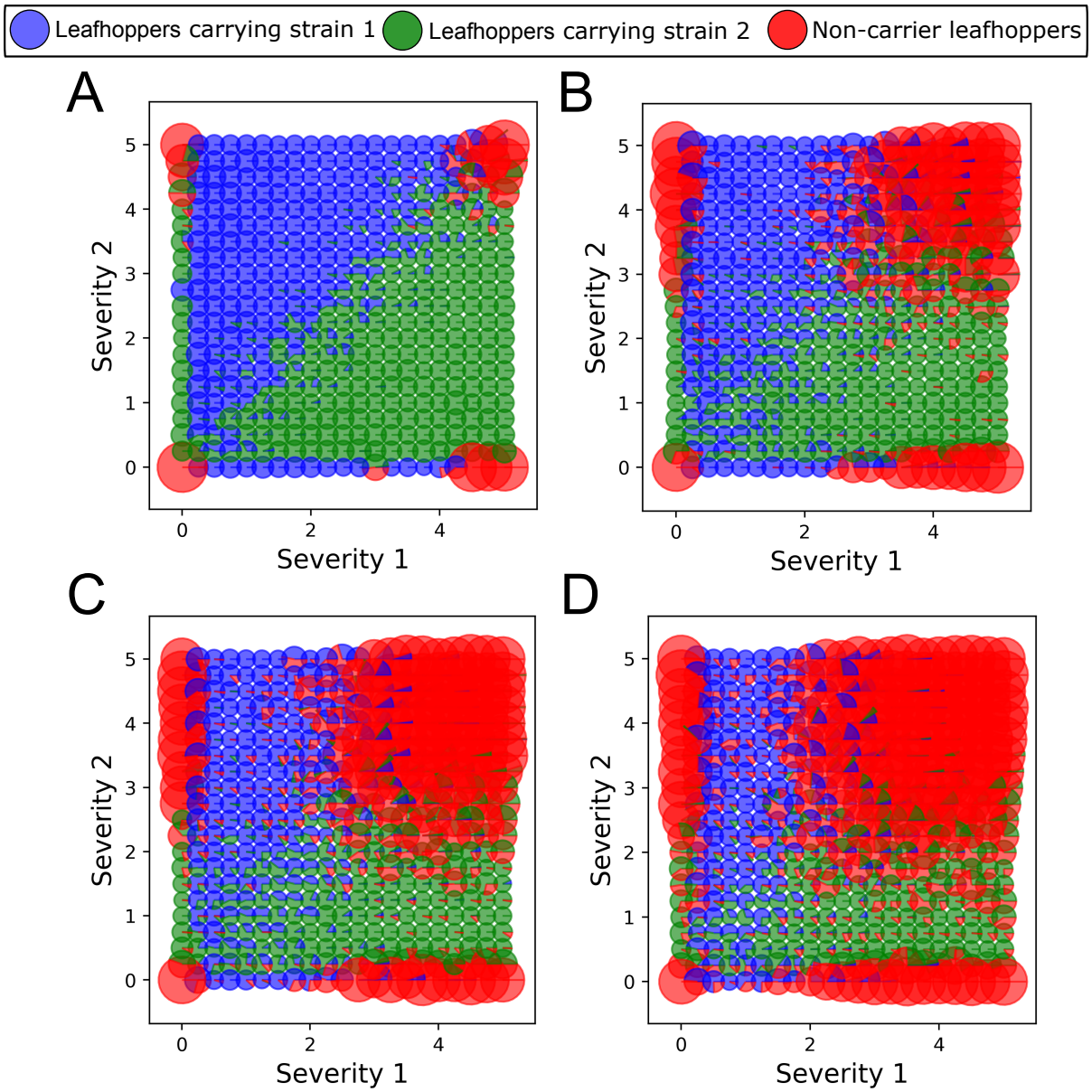

Figure S7. The impact on the evolutionary dynamics of the leafhopper movement. Outcome of competition experiments for (A) $s = 2.9\,\mathrm{m\,d^{-1}}$; (B) $s = 3.0\,\mathrm{m\,d^{-1}}$; (C) $s = 3.1\,\mathrm{m\,d^{-1}}$; (D) $s = 3.2\,\mathrm{m\,d^{-1}}$.

Supplemental References

B. G. Akre and D. M. Johnson. Switching and sigmoid functional response curves by damselfly naiads with alternative prey available. *The Journal of Animal Ecology*, pp. 703–720 (1979).

R. M. Anderson and R. M. May. Coevolution of hosts and parasites. *Parasitology*, 85(2):411–426 (Oct 1982). ISSN 1469-8161, 0031-1820. doi:10.1017/S0031182000055360.

W. J. Bell. *Searching behaviour: the behavioural ecology of finding resources*. Springer Science & Business Media, Dordrecht (2012).